Research Article

Li Pinjun, Xiong Zhengye*, Ma Zidong, Guo Jingyuan, and Wang Chunxi

Analysis of Cu and Zn contents in aluminum alloys by femtosecond laser-ablation spark-induced breakdown spectroscopy

https://doi.org/10.1515/phys-2023-0113
received April 09, 2023; accepted September 02, 2023

Abstract: To enhance the sensitivity of detecting Cu and Zn in aluminum alloys, we incorporated a spark discharge unit into the femtosecond laser-induced breakdown spectroscopy (fs-LIBS) system, forming a femtosecond laser ablation spark-induced breakdown spectroscopy (fs-LA-SIBS) system. We utilized both fs-LA-SIBS and fs-LIBS techniques to detect Cu and Zn in various aluminum alloy samples with different contents. Our results reveal that the spark discharge extends the duration of laser-induced plasma atomic radiation and amplifies the peak intensity of atomic radiation, thereby significantly increasing the time-integrated signal intensity of laser-induced plasma. Under the present experimental conditions, the limits of detection (LoDs) of Cu and Zn in aluminum alloy by fs-LA-SIBS are 16 and 12 ppm, respectively. In contrast, the LoDs of Cu and Zn by fs-LIBS technique under the same laser pulse energy are 96 and 84 ppm, respectively. Hence, for Cu, the LoDs by the fs-LA-SIBS technique are 1/6 of those by the fs-LIBS technique, and for Zn, the LoDs by the fs-LA-SIBS technique are 1/7 of those by the fs-LIBS technique. Our findings demonstrate that the fs-LA-SIBS technique is more sensitive than the fs-LIBS technique in the quantitative analysis of elements and may be a practical approach for elemental analysis in alloys.

Keywords: laser-induced breakdown spectroscopy, laser-ablation spark-induced breakdown spectroscopy, aluminum alloy, detection technology

*** Corresponding author: Xiong Zhengye**, School of electronic and Information Engineering, Guangdong Ocean University, Zhanjiang, 524088, China, e-mail: xiongzhengye@139.com
Li Pinjun: Department of Information Science, ZhanJiang Preschool Education College, ZhanJiang 524084, China, e-mail: pingyuejushi@126.com
Ma Zidong, **Guo Jingyuan**, **Wang Chunxi:** School of electronic and Information Engineering, Guangdong Ocean University, Zhanjiang, 524088, China

1 Introduction

Laser ablation (LA) technology uses pulsed lasers to rapidly heat a localized area on a sample surface, creating a transient plasma that provides a good basis for spectroscopic analysis [1,2]. Laser-induced breakdown spectroscopy (LIBS) has made significant progress in element analysis in various fields over the past few decades [3–5]. Los Alamos National Laboratory *et al.* have developed the ChemCam LIBS instrument onboard Curiosity which can be used to both identify and analyze rock surface alteration features [6–8], and the Chinese-developed Mars rover "Zhurong" successfully landed on the Martian surface carrying a surface composition detector which uses LIBS technology in 2021 [9]. The most commonly used laser in the LIBS system is a Q-switched Nd:YAG laser with pulse widths ranging from a few nanoseconds to over a hundred nanoseconds. The wide pulse range makes the interaction between laser and matter very complex. In contrast, ultrashort pulse lasers such as femtosecond (fs) lasers exhibit a series of advantages in their interaction with matter [10]. Therefore, LIBS with fs laser, that is, femtosecond laser-induced breakdown spectroscopy (fs-LIBS), has gradually become the mainstream of LIBS [11]. fs-LIBS is especially suitable for 2D surface analysis with high lateral resolution, 3D element mapping analysis, depth profile study with high depth resolution, and biological sample analysis with less damage [12–14]. Early studies of fs-LIBS showed that the intensity of line emission and continuous background spectrum and the temperature of plasma decrease rapidly after laser excitation. Since the duration of line emission is usually less than 1 μs [15], time-resolved signal detection is required to improve analysis sensitivity [16]. Although intensified charge-coupled device detectors have the advantages of fast gating and high detection sensitivity, the cost of these detectors is usually high.

To improve the signal intensity of laser-induced plasma, dual-pulse LIBS (DP-LIBS) technology has developed [17]. There are usually two types of DP-LIBS: one is based on

two fs laser pulses, namely fs-fs DP-LIBS, and the other is based on the combination of fs and nanosecond laser pulses, namely fs-ns DP-LIBS. In fs-ns DP-LIBS, the fs laser pulse is used as the ablation laser, and the nanosecond laser pulse is used as the reheating laser, and they are arranged orthogonally. The signal is enhanced and can reach hundreds of times [18].

Although fs-ns DP-LIBS can achieve high signal enhancement factors, in some cases, there is a need to operate LIBS at a high repetition rate due to requirements for data acquisition speed or size limitations of the spectrometer. Nanosecond lasers that operate at high repetition rates have very low pulse energy, resulting in a lower practical signal enhancement factor in fs-ns DP-LIBS under such conditions. Therefore, it is necessary to find a suitable method to enhance the plasma emission signal of high-repetition-rate fs-LIBS. Spark discharge can effectively enhance laser-induced plasma emission. This discharge can be triggered by laser-induced plasma [19] or external discharge methods [20]. The start time of spark discharge is controlled by a quick switch, or the start time and pulse width are controlled by a gated high-voltage power supply. Spark discharge can operate at a high repetition rate and obtain a strong elemental spectrum signal. This mechanism of spark discharge-assisted signal enhancement is also known as spark-induced breakdown; hence, the LIBS enhanced by fs LA and spark-induced breakdown spectroscopy (fs-LA-SIBS) are referred to as fs-LA-SIBS.

Aluminum alloys are widely used in daily life and industrial production. Many aluminum alloys contain elements Cu and Zn [21]. The physical properties of aluminum alloys with different compositions vary greatly, such as ADC12 being suitable for making die castings [22] and A356 having high corrosion resistance [23]. There are clear regulations on the content of Cu and Zn in aluminum alloys of different grades. Therefore, by accurately measuring the content of Cu and Zn in aluminum alloys, it is possible to determine the type and quality of aluminum alloy material. In this article, the spark discharge is applied as a signal enhancement method in fs-LIBS with a pulse repetition frequency of 1 kHz, and the limits of detection (LoDs) and other analytical performance parameters of copper and zinc in several aluminum alloy samples are evaluated and discussed.

2 Experimental methods

The experimental setup for fs-LA-SIBS is shown in Figure 1. A Ti:Sapphire laser (Astrella, Coherent Inc., USA) was used as the ablation laser source, with a pulse width of 35 fs, a maximum output pulse energy of 6 mJ, and a repetition rate of 1 kHz. The laser wavelength used in the experiment was 800 nm, and the output laser beam diameter was 10 mm. The laser beam was tightly focused on the sample surface (numerical aperture: 0.25, working distance: 15 mm) through 10 high-power focusing lenses (LMU-10X-266, Thorlabs Inc., USA) to ablate the sample and generate the laser-induced plasma. In the experiment, a polarizer and an aperture were used to attenuate the pulse energy to less than 1.0 mJ.

As shown in Figure 1, the energy of the laser pulse was adjusted by rotating the angle between two Glan-Taylor polarizers. The residual laser was received by a fast photodiode after passing through a beamsplitter (BS) and converted into a corresponding electrical signal, which served

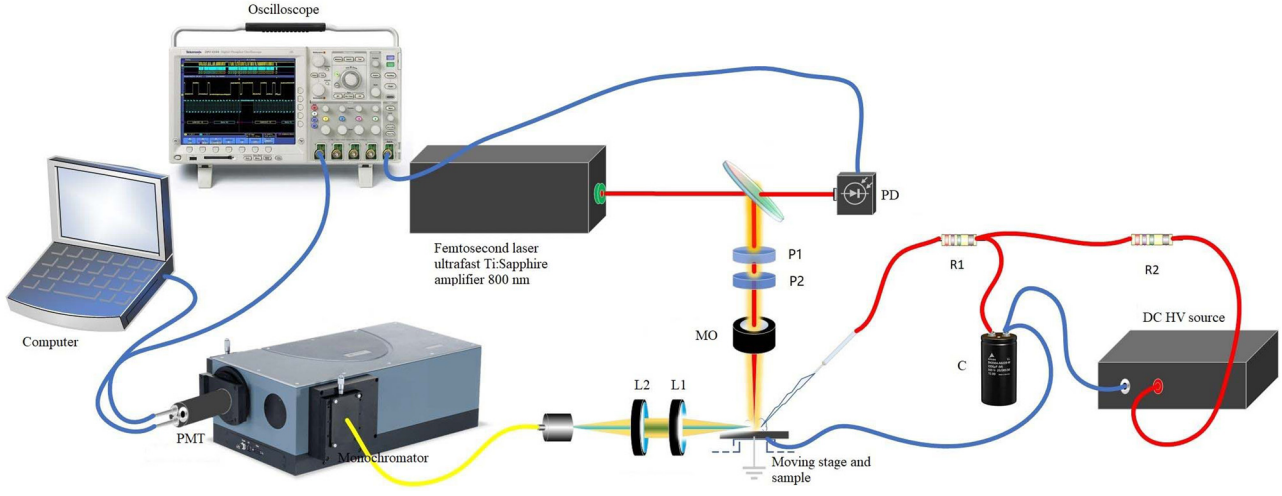

Figure 1: Setup of fs-LA-SIBS.

as a synchronous trigger signal for monitoring ion emission by using an oscilloscope. The percentage of the residual laser signal after passing through the BS is about 20%. The aluminum alloy sample was fixed on a two-dimensional X–Y moving platform. During the experiment, the platform maintained a movement speed of 2 mm/s to ensure that the surface hit by each laser pulse was new. A ceramic plate was placed between the sample and the platform to keep the sample electrically insulated from the platform.

Figure 1 also shows the spark discharge device used for spark-induced breakdown. A DC power supply (4 kV, 50 mA) charges the high voltage capacitor C (5 nF) through the current limiting resistor R2 (80 kΩ). The anode of the spark discharge is a tungsten needle with a diameter of 2 mm, while the cathode is the tested aluminum alloy sample plate. The tip of the anode tungsten wire is polished into a cone shape and installed on the sample surface at a 45° angle. Once the fs laser pulse generates plasma, the gap resistance between the tip of the tungsten wire and the sample surface will immediately decrease, thus producing a spark discharge at the same repetition frequency as the laser pulse. The electric energy stored in the capacitor is released into the laser-induced plasma through the current limiting resistor R1 (4 Ω), further decomposing the ablated sample and enhancing the atomic emission spectrum intensity of the plasma.

The plasma radiation was collected by a lens system and focused onto the input port of a fiber optic spectrometer for spectral analysis. A monochromator (Omni-λ3017i, Zolix Inc., CN) was used to select the emission line for analysis, and a 500 MHz digital storage oscilloscope (GDS3502, GW Inc., CN) was used to record the output signal of the photomultiplier tube. The data stored in the oscilloscope were transferred to a personal computer for further processing. A multi-channel fiber optic spectrometer (1202156U3, 1202157U3, and 1202158U3, Avantes Inc., NLD) was used to record the spectrum in the wavelength range of 200–500 nm. The fiber optic spectrometer includes three channels, which cover the wavelength ranges of 200–317, 317–415, and 415–500 nm, respectively. Each channel's linear charge-coupled device (CCD) detector has 2,048 pixels, and the spectral resolution of these channels is less than 0.1 nm.

Table 1: Contents of Cu and Zn in standard aluminum alloy samples (wt%)

Sample no.	GB215	GB216	GB217	GB218	GB219
Contents of Zn	0.011	0.046	0.089	0.140	0.200
Contents of Cu	0.190	0.150	0.100	0.053	0.016
Aluminum	98.639	98.843	99.062	99.257	99.360

Before applying fs-LA-SIBS technology to analyze the content of Cu and Zn in aluminum alloys, it is necessary to establish a standard curve using standard samples. In this study, five different standard samples (being purchased from Fushun Aluminum Factory Standard Sample Research Institute, China) with varying Cu and Zn contents (as shown in Table 1) were used to establish the standard curves for different trace elements, and the LoDs were also evaluated.

3 Results and discussion

3.1 Signal enhancement observation

The emission spectra of Al exhibit peaks at 390.1, 394.4, 396.2, and 466.3 nm [24]. To compare the enhancement effect of spark-induced breakdown on the spectra, plasma radiation at 394.4 and 393.0 nm was monitored under two

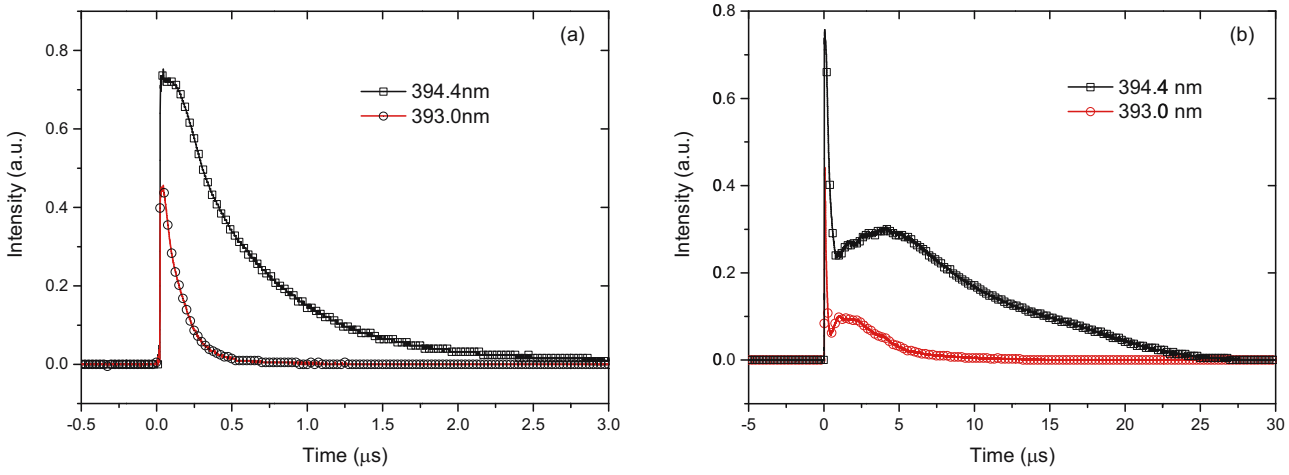

Figure 2: Time domain diagram of plasma emission at 394.4 and 393.0 nm in (a) fs-LIBS and (b) fs-LA-SIBS, respectively. The laser pulse energy is 0.4 mJ and the discharge voltage is 1.6 kV.

different excitations (as shown in Figure 2): fs-LIBS and fs-LA-SIBS. The first excitation is generated by fs laser pulse-induced breakdown, while the second excitation is generated by fs-LA-SIBS. The spectrum at 393.0 nm is close to the Al I 394.4 nm line and can be used to evaluate the continuous spectrum background. Al ion radiation and continuous background can be observed at 394.4 nm, while only continuous background can be observed at 393.0 nm. The following parameters were selected to record these results: pulse energy of 0.4 mJ, capacitor of 5 nF, and discharge voltage of 1.6 kV, as shown in Figure 2.

Figure 2 shows that under fs-LIBS excitation conditions (Figure 2(a)), the atomic radiation of Al at 394.4 nm lasts less than 2.15 μs, and the continuum background at 393.0 nm lasts less than 0.43 μs. Therefore, for time-resolved signal detection in fs-LIBS, the time window of the data acquisition gate was set to 0.43–2.15 μs. Under fs-LA-SIBS excitation conditions (Figure 2b), the duration of atomic emission of Al at 394.4 nm is extended to 22.5 μs, and the duration of the continuum background at 393.0 nm is extended to 5.5 μs. For time-resolved signal detection in fs-LA-SIBS, the time window of the data acquisition gate was set to 5.5–22.5 μs, and the time-integrated signal intensity was significantly enhanced. It can be seen that the extension of the duration of the spark-induced breakdown plasma emission makes it easier to achieve time-resolved signal detection.

Plasma emission spectra generated by fs-LIBS and fs-LA-SIBS in non-gated mode of operation were recorded with an AVANTES multi-channel spectrometer, the sample analyzed was standard aluminum alloy GB216. Figure 3a shows the emission spectra in the wavelength range of 260–500 nm recorded by fs-LIBS and fs-LA-SIBS operating at a repetition rate of 1 kHz. The laser pulse energy and high voltage for spark discharge were the same as mentioned earlier. The integration time of the spectrometer was 20 ms, *i.e.*, an average of 20 discharges was accumulated for each measurement.

From Figure 3, it can be seen that the spectra recorded by the fs-LA-SIBS technique are significantly enhanced compared to those recorded by the fs-LIBS technique. For example, in the fs-LIBS spectra, the emission intensity at 466.3 (spectrum of Al plasma emission) nm is about 3.5×10^4, much higher than that in the fs-LA-SIBS spectrum (about 1.1×10^4). In the fs-LIBS spectrum, the intensity of emissions from Cu ions at 324.8 nm is about 390, and that from Zn ions at 334.5 nm is about 480, while in the fs-LA-SIBS spectrum, the corresponding emissions from Cu ions and Zn ions are about 0.85×10^4 and 1.20×10^4 (Figure 3b).

3.2 Comparison of LoDs

To evaluate the analytical sensitivity of fs-LA-SIBS technology and compare it with fs-LIBS technology, LoDs of Cu and Zn elements in aluminum alloys were selected for comparison. The LoD of an element was determined using the widely accepted 3σ rule [25], that is:

$$\mathrm{LoD} = \frac{3\sigma_B}{S}, \tag{1}$$

where σ_B is the standard deviation (SD) of the background and S is the slope of the calibration curve.

Figures 4 and 5 show the calibration curves for Cu and Zn, respectively, elements in aluminum alloys obtained using fs-LIBS and fs-LA-SIBS technologies, and the data are listed in Table 2. In the experiments, the pulse energy of the fs laser was set to 0.4 mJ, the discharge voltage was 1.6 kV, the capacitance was 5 nF, and the CCD in the fiber spectrometer was set to an integration time of 20 ms. The

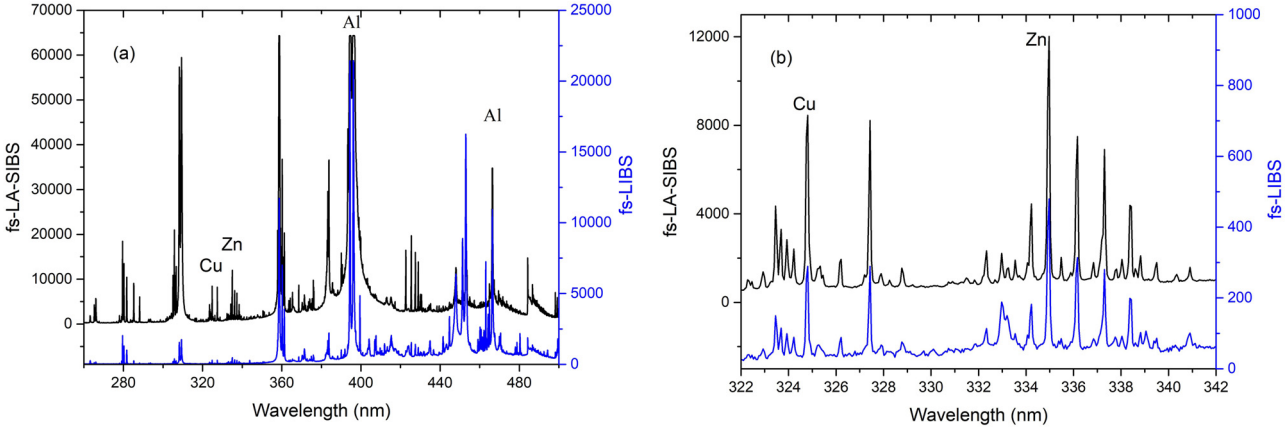

Figure 3: Plasma emission spectra recorded in fs-LIBS and fs-LA-SIBS, respectively. (a) Spectra in the wavelength range of 260–500 nm; (b) Spectra in the wavelength range of 322–342 nm.

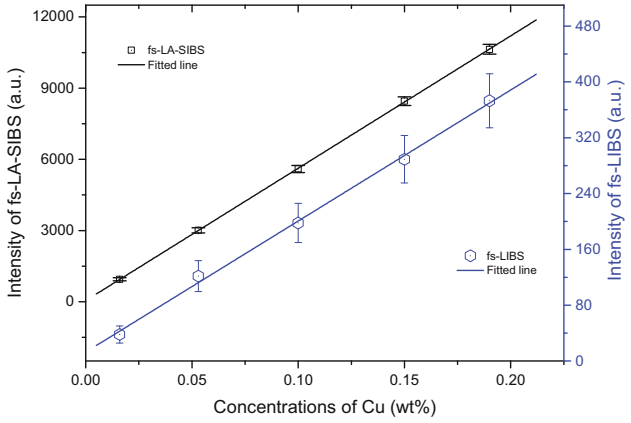

Figure 4: Calibration curves of cuprum in aluminum alloy by fs-LA-SIBS and fs-LIBS.

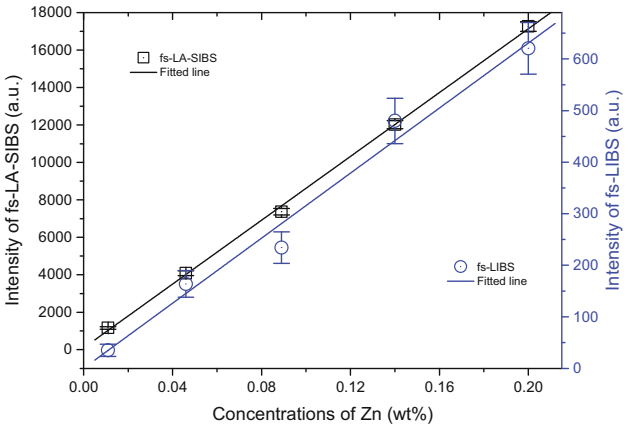

Figure 5: Calibration curves of zinc in aluminum alloy by fs-LA-SIBS and fs-LIBS.

final spectrum was the average of 20 overlapped spectra, and the net peak height of the analysis line was used as the signal intensity. The selected spectral lines were the emission lines of Cu ions at 324.8 nm and Zn ions at 334.5 nm, with errors determined from the signal deviation of 10 measurements.

From these figures and Table 2, it can be seen that although the SD of the data points corresponding to the calibration curve obtained by the fs-LA-SIBS technique was larger than that obtained by the fs-LIBS technique, the relative deviation was much smaller than that of the fs-LIBS technique. The standard curve was obtained by fitting the measured data points using the least-squares method, with the fitted parameters listed in Table 3. To evaluate the LoD, the SD of the background corresponding to the analysis line, σ_B, is needed. Here, σ_B was evaluated based on the SD of the background in a 1-nm wavelength range near the analysis line. Table 3 lists the corresponding background SD σ_B and the LoDs of copper and zinc elements calculated by formula (1).

As shown in Table 3, the LoDs of Cu and Zn obtained by the fs-LA-SIBS technique were only about 1/6 to 1/7 of those obtained by the fs-LIBS technique, indicating a significantly improved detection sensitivity. Due to the interaction between spark discharge and laser-induced plasma, the signal emitted by the plasma could be enhanced, thereby increasing the analytical sensitivity. Therefore, the fs-LA-SIBS technique could be a highly useful elemental analysis technique and may have widespread applications.

Table 2: The data corresponding to the calibration curve obtained by the fs-LA-SIBS and the fs-LIBS techniques

Conc. of Cu (wt%)	Mean counts of fs-LA-SIBS	SD	Relative deviation (%)	Mean counts of fs-LIBS	SD	Relative deviation (%)
0.016	946	62	6.5	38.1	12.3	32.4
0.053	3,002	110	3.7	121.8	22.1	18.1
0.100	5,594	150	2.7	197.9	28.1	14.2
0.150	8,452	184	2.2	289.2	34.0	11.8
0.190	10,632	206	1.9	372.9	38.6	10.4

Table 3: LoDs of cuprum and zinc in aluminum alloy obtained by fs-LIBS and fs-LA-SIBS techniques

		Intercept distance	Slop/100	Determination coefficient (R)	σ_B	LOD (ppm)
Cu	fs-LA-SIBS	45 ± 25	55,790 ± 211	0.99994	29	16
	fs-LIBS	12 ± 6	1,878 ± 52	0.99700	6	96
Zn	fs-LA-SIBS	95 ± 166	85,219 ± 1,403	0.99892	33	12
	fs-LIBS	−1 ± 24	3,176 ± 204	0.98361	9	85

4 Conclusion

In this study, trace elements copper and zinc in aluminum alloy samples were detected and analyzed using an fs-LA-SIBS system with a repetition rate of 1 kHz. Compared with the fs-LIBS technique, the assistance of spark discharge can significantly enhance the atomic emission intensity of laser-induced plasma, resulting in a much higher sensitivity of fs-LA-SIBS. Under the experimental conditions, the LoDs of copper and zinc elements in an aluminum alloy using fs-LA-SIBS were 16 and 12 ppm, respectively, which were only about 1/6 to 1/7 of the LoDs obtained by the fs-LIBS method without spark discharge. The high sensitivity of fs-LA-SIBS makes it a promising technique for the analysis of elements in alloys.

Acknowledgments: The authors would like to acknowledge helpful discussions with Dr. He Xiaoyong of Dongguan University of Technology, et al.

Funding information: This work was supported by Special Innovation Projects of General Universities in Guangdong Province, China(2020KTSCX351), Science and Technology Planning Project of Guangdong Province, China(2015A020216020), the Education and Teaching Research Project of Guangdong Ocean University (S2020105666059), and Research Foundation for Talented Scholars of Guangdong Ocean University (060302112102).

Author contributions: All authors have accepted responsibility for the entire content of this manuscript and approved its submission.

Conflict of interest: The authors state no conflict of interest.

Data availability statement: The data that support the findings of this study are available from the corresponding author upon reasonable request.

References

[1] Russo RE, Mao X, Liu H, Gonzalez J, Mao SS. Laser ablation in analytical chemistry: A review. Talanta. 2002;57(3):425–51.
[2] Ye H, Zhang J, Mei H, Huang Y, Yuan Z, Cao Z, et al. Quantitative analysis of aluminum in alloy Steel by laser ablation absorption spectroscopy. Chin J Lasers. 2020;47(10):299–305.
[3] He X, Chen B, Chen Y, Li R, Wang F. Femtosecond laser-ablation spark-induced breakdown spectroscopy and its application to the elemental analysis of aluminum alloys. J Anal Atom Spectrom. 2018;33(12):2203–9.
[4] Liu S, Xiu J, Liu Y. Rapid quantitative analysis of element content ratios in Cu(In,Ga)Se_2 thin films using laser-induced breakdown spectroscopy. Chin J Lasers. 2019;46(9):0911001.
[5] Sabsabi M, Cielo P. Ouantitative analysis of aluminum alloys by laser-induced breakdown spectroscopy and plasma characterization. Appl Spectrosc. 1995;49(4):499–507.
[6] Fabre C, Maurice S, Cousin A, Wiens RC, Forni O, Sautter V, et al. Onboard calibration igneous targets for the Mars Science Laboratory Curiosity rover and the Chemistry Camera laser induced breakdown spectroscopy instrument. Spectrochim Acta Part B At Spectrosc. 2011;66:280–9.
[7] Lanza NL, Ollila AM, Cousin A, Wiens RC, Clegg S, Mangold N, et al. Understanding the signature of rock coatings in laser-induced breakdown spectroscopy data. Icarus. 2015;249:62–73.
[8] Anderson RB, Forni O, Cousin A, Wiens RC, Clegg SM, Frydenvang J, et al. Post-landing major element quantification using SuperCam laser induced breakdown spectroscopy. Spectrochim Acta Part B At Spectrosc. 2022;188:106347.
[9] Yang JF, Liu DW, Xue B, Lyu J, Liu JJ, Li F, et al. Design and ground verification for multispectral camera on the mars tianwen-1 rover. Space Sci Rev. 2022;218(3):1–27.
[10] Jiang Z, Kieffer J, Xu Z. Intense ultrafast laser-matter interaction and its application. Chin J Lasers. 1996;23(6):513–9.
[11] Santagata A, De Bonis A, Villani P, Teghil R, Parisi GP. Fs/ns-dual-pulse orthogonal geometry plasma plume reheating for copper-based-alloys analysis. Appl Surf Sci. 2006;252(13):4685–90.
[12] Choi JH, Shin S, Moon Y, Han JH, Hwang E, Jeong S. High spatial resolution imaging of melanoma tissue by femtosecond laser-induced breakdown spectroscopy. Spe Acta Part B At Spectrosc. 2021;179:106090.
[13] Ma S, Gao X, Guo K, Kahsay M, Lin J. Analysis of the element content in poplar tree leaves by femtosecond laser-induced breakdown spectroscopy. Sci China Phys Mech. 2011;54(11):1953–7.
[14] de Carvalho GG, Moros J, Santos Jr D, Krug FJ, Laserna JJ. Direct determination of the nutrient profile in plant materials by femtosecond laser-induced breakdown spectroscopy. Anal Chim Acta. 2015;876:26–38.
[15] Eland KL, Stratis DN, Gold DM, Goode SR, Angel SM. Energy dependence of emission intensity and temperature in a LIBS plasma using femtosecond excitation. Appl Spectrosc. 2001;55(3):286–91.
[16] Guido RC, Pedroso F, Contreras RC, Rodrigues LC, Guariglia E, Neto JS. Introducing the Discrete Path Transform (DPT) and its applications in signal analysis, artefact removal, and spoken word recognition. Digit Signal Process. 2021;117(11):103158.
[17] Marangoni BS, Nicolodelli G, Senesi GS, fonseca N, Izario Filho HJ, Xavier AA, et al. Multi-elemental analysis of landfill leachates by single and double pulse laser-induced breakdown spectroscopy. Microchem J. 2021;165:106125.
[18] Yang R, Bi L. Spectral enhancement mechanism and analysis of defocused collinear DP-LIBS technology. Optik. 2021;243:167025.
[19] He X, Li R, Chen Y. Application of fiber optic high repetition rate laser-ablation spark-induced breakdown spectroscopy on the elemental analysis of aluminum alloys. Appl Opt. 2019;58(31):8522–8.
[20] Gao J, Kang J, Li R, Chen Y. Application of calibration-free high repetition rate laser-ablation spark-induced breakdown spectroscopy for the quantitative elemental analysis of a silver alloy. Appl Opt. 2020;59(13):4091–6.
[21] Guo X, Li H, Pan Z, Zhou S. Microstructure and mechanical properties of ultra-high strength Al-Zn-Mg-Cu-Sc aluminum alloy

fabricated by wire + arc additive manufacturing. J Manuf Process. 2022;79:576–86.
[22] Yun X, Wang Z, Gardner L. Full-range stress–strain curves for aluminum alloys. J Struct Eng. 2021;147(6):04021060.
[23] Jeon JH, Jeon JG, Joo MR, Lee JW, Bae DH. Deformation behavior of an A356 alloy containing small sub-grains with wide low-angle boundary. J Alloy Compd. 2022;908:164550.
[24] Cong R, Zhang BH, Fan JM, Zheng XF, Liu WQ, Zheng RE, et al. Experimental investigation on time and spatial evolution of emission spectra of Al atom in laser-induced plasmas. Acta Opt Sin. 2009;29(9):2594–600.
[25] Ma S, Guo L, Dong D. A molecular laser-induced breakdown spectroscopy technique for the detection of nitrogen in water. J Anal Atom Spectrom. 2022;37:663–7.